

Path-following Approach to Control Effort Reduction of Tracking Feedback Laws

Dragan B. Dačić, Maksim V. Subbotin and Petar V. Kokotović

Abstract—We develop a path-following algorithm for re-design of tracking feedback laws to reduce the control effort. Our algorithm provides a tradeoff between the control effort and the dynamic performance along the path, while maintaining the desired convergence to the path. It is applicable to feedback linearizable systems with stable zero dynamics. We illustrate it on a realistic hovercraft model, and compare the resulting control effort with control efforts of other path-following and tracking algorithms.

I. INTRODUCTION

Several path-following and maneuvering problems have recently been formulated to replace the standard reference tracking problem as more suitable for certain applications [1], [2], [3], [4]. The primary interest in these applications is to solve the *geometric task*, that is, to steer an object (vehicle, airplane, robot arm, etc.) to reach and follow a desired geometric path $\mathcal{Y}_p \triangleq \{y_p(\theta) \in \mathbb{R}^m : \theta \in \mathbb{R}\}$. A secondary objective, the *dynamic task*, is to force the object moving along the path \mathcal{Y}_p to satisfy a dynamic specification. The design of path-following and maneuvering feedback laws suppresses the time-dependence of the motion by parameterizing the path \mathcal{Y}_p with an auxiliary variable θ . A feedback law for the original control variable u is constructed to satisfy the geometric task, leaving θ to be designed as a function of time and system state to fulfill the dynamic task.

In our interpretation of path-following we introduce a fictitious object, called the leader. The leader moves along \mathcal{Y}_p , and its position on \mathcal{Y}_p at time t is $\theta(t)$. Then the geometric task is to design a feedback law for u which ensures that the physical object, called the follower, asymptotically converges to the leader for any admissible leader's motion. The dynamic task is to design a feedback law for θ which guarantees that leader's motion satisfies the dynamic specification. Path-following is more flexible than reference tracking where leader's motion $\theta(t)$ is predetermined $\forall t \geq 0$.

In this paper we use the freedom to design $\theta(t)$ to achieve a reduction of control effort measured by either magnitude or energy of the control variable. It was observed in several papers [1], [3], [4] that path-following feedback law usually results in lower control effort than the corresponding tracking feedback law, but there are no systematic procedures which guarantee this reduction.

This work is supported by NSF under grants ECS-9812346 and ECS-0218226.

Dragan B. Dačić is with Department of Electrical and Electronic Engineering, The University of Melbourne, Victoria 3010 Australia, d.dacic@ee.unimelb.edu.au; Maksim V. Subbotin and Petar V. Kokotović are with Center for Control, Dynamic Systems and Computation, University of California, Santa Barbara, CA 93106-9560, USA, subbotin@engineering.ucsb.edu, petar@ece.ucsb.edu.

Our path-following design implements a gradually changing tradeoff between the dynamic task and follower's control effort. We start with a tracking feedback law which enforces the desired convergence to a given reference signal. Using the corresponding path-following feedback law to control the follower, we maintain follower's desired convergence to the path. Then we construct a feedback law for leader's motion $\theta(t)$ to reduce follower's control effort. As the leader-follower distance decreases, leader's feedback law gives higher priority to the dynamic task.

The main contribution of this paper is the algorithm for design of leader's feedback law. In this algorithm we compute leader's feedback law by pointwise minimizing the sum of two terms. The first term measures follower's control effort due to the geometric error between the leader and the follower, while the second term measures the deviation of leader's motion from the given dynamic specification. Relative weights of these terms trade follower's control effort for its dynamic performance along the path. Our algorithm is applicable to nonlinear systems with uniform vector relative degree and stable zero dynamics. While the assumption on uniformity of the vector relative degree can be relaxed by resorting to dynamic extension [5] and dynamic reduction [8], the assumption on stability of zero dynamics can not, since it represents a necessary condition for asymptotic tracking of an open set of reference signals [9].

We start with a motivating example in Section II. For systems with uniform vector relative degree we develop our path-following algorithm in Section III. The modifications of the algorithm for systems with nonuniform vector relative degree are presented in Section IV. We apply our path-following algorithm to a realistic hovercraft model in Section V and give concluding remarks in Section VI.

Given a function of time $f : \mathbb{R}^n \rightarrow \mathbb{R}^m$, we write $f^{(i)}$ for its i^{th} time derivative, $f^{(i)} \triangleq \frac{d^i f(t)}{dt^i}$. We denote the identity matrix $I_n \in \mathbb{R}^{n \times n}$, and a diagonal matrix $D \in \mathbb{R}^{k \times k}$ whose diagonal entries are $D_i \in \mathbb{R}^{m \times m}$, $i = 1, \dots, k$, and all other entries are zeros by $D \triangleq \text{diag}(D_1, \dots, D_k)$. We define matrices $C_r \triangleq [1 \dots 0 \ 0] \in \mathbb{R}^{1 \times r}$, $B_r^T \triangleq [0 \dots 0 \ 1] \in \mathbb{R}^{1 \times r}$, $A_r \triangleq \begin{bmatrix} 0 & I_{r-1} \\ 0 & 0 \end{bmatrix} \in \mathbb{R}^{r \times r}$, and matrices $C_{r,m} \triangleq \text{diag}(C_r, \dots, C_r)$, $A_{r,m} \triangleq \text{diag}(A_r, \dots, A_r)$, $B_{r,m} \triangleq \text{diag}(B_r, \dots, B_r)$, where the second index m denotes the number of diagonal entries.

II. MOTIVATING EXAMPLE

To motivate our approach to control effort reduction we consider an LQ optimal tracking feedback law, and discuss

the tradeoff between the convergence rate and the control effort. Then we compare these results with the results obtained via our path-following algorithm developed in Section III.

Example 1: For the system

$$\ddot{x}_1 = u_1, \quad \ddot{x}_2 = u_2, \quad x_i, u_i \in \mathbb{R}, \quad i = 1, 2, \quad (1)$$

we design a feedback law to force the output $y \triangleq x$ to asymptotically track the reference signal $y_T(t) \triangleq [y_{T1}(t) \ y_{T2}(t)]^T$. Introducing the error coordinates $e_T \triangleq [x_1 - y_{T1} \ \dot{x}_1 - \dot{y}_{T1} \ x_2 - y_{T2} \ \dot{x}_2 - \dot{y}_{T2}]^T$ into system (1) we get

$$\dot{e}_T = A_{2,2}e_T + B_{2,2}(u - \ddot{y}_T). \quad (2)$$

The tracking feedback law, designed by minimizing $J = \int_0^\infty (e_T^T(t)Qe_T(t) + \tilde{u}^T(t)R\tilde{u}(t)) dt$, $Q = \text{diag}(q, 0, q, 0)$, where $\tilde{u} \triangleq u - \ddot{y}_T$, $R = \text{diag}(r, r)$, $q, r > 0$, is

$$u = \kappa_g(e_T) + \ddot{y}_T, \quad \kappa_g(e_T) \triangleq -R^{-1}B^T P e_T, \quad (3)$$

where $P = P^T > 0$ is the solution of the algebraic Riccati equation $A_{2,2}^T P + P A_{2,2} + Q - P B_{2,2} R^{-1} B_{2,2}^T P = 0$.

We show the closed-loop behavior for two sets of penalties $q = 100$, $r = 10$, and $q = 100$, $r = 300$, in Figs. 1a, 1b, respectively. In Fig. 1a, $y(t)$ quickly converges to $y_T(t) = R[\sin(v_0 t) \ \cos(v_0 t)]^T$, but the control effort, Fig. 1d, is large. By increasing r , Fig. 1b, we reduce the control effort, but slow down the convergence. This is the familiar tradeoff provided by the LQ methodology.

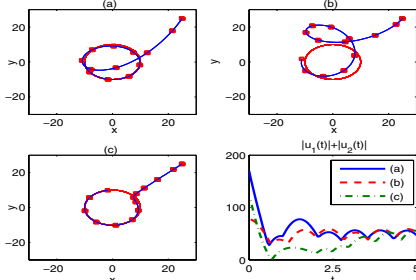


Fig. 1. Output values $y(t_i)$, $t_i = 0.4i$, for: (a) feedback law (3), $q = 100$, $r = 10$, (b) feedback law (3), $q = 100$, $r = 300$, (c) feedback law (6), $q = 100$, $r = 10$, $\omega = \sigma(e_P, \theta, \dot{\theta})$, and (d) pointwise norm of control signals, $|u_1(t)| + |u_2(t)|$.

In Fig. 1c we show a noticeable improvement achieved by exploiting the additional flexibility of path-following. Substituting $y_P(\theta) = R[\sin \theta \ \cos \theta]^T$ and $e_P \triangleq [x_1 - y_{P1} \ \dot{x}_1 - \dot{y}_{P1} \ x_2 - y_{P2} \ \dot{x}_2 - \dot{y}_{P2}]^T$ into (1), we get

$$\dot{e}_P = A_{2,2}e_P + B_{2,2}(u - \ddot{y}_P), \quad (4)$$

$$\dot{\theta} = \omega. \quad (5)$$

A distinguishing feature of path-following is that $\ddot{y}_P = \frac{\partial^2 y_P}{\partial \theta^2} \dot{\theta}^2 - \frac{\partial y_P}{\partial \theta} \ddot{\theta}$ gives rise to two new states, $[\theta \ \dot{\theta}]^T$, and $\theta = \omega$ is an additional control input in augmented system (4)–(5). Here, subsystem (4) governs the geometric error between the leader and the follower, while subsystem (5) represents leader's dynamics. We let follower's feedback law

$$u = \kappa_g(e_P) + \ddot{y}_P, \quad \ddot{y}_P = \frac{\partial^2 y_P}{\partial \theta^2} \dot{\theta}^2 - \frac{\partial y_P}{\partial \theta} \omega, \quad (6)$$

enforce the geometric task. With so determined $\kappa_g(e_P)$ we design leader's feedback law $\omega = \sigma(e_P, \theta, \dot{\theta})$ to reduce the

control effort of feedback law (6) and enforce the dynamic task $\lim_{t \rightarrow \infty} \dot{\theta}(t) = v_0$, where v_0 is the desired speed.

We say that path-following feedback law (6) corresponds to tracking feedback law (3) because it is obtained by replacing e_T with e_P and y_T with y_P . Consequently feedback laws (3) and (6) achieve the same rate of convergence of $e_P(t)$ and $e_T(t)$ to zero, while the freedom to design ω allows us to further reduce the control effort of feedback law (6). The price paid for this reduction is slower convergence of $\dot{\theta}(t)$ to v_0 . Thus, path-following framework enables to maintain the desired rate of convergence to the geometric path, while providing the tradeoff between the control effort and the dynamic performance along the path.

In Fig. 1c we show the typical behavior using (6) with $q = 100$, $r = 10$, and $\omega = \sigma(e_P, \theta, \dot{\theta})$ designed in Section III. The resulting output trajectory has two phases. In the first phase $y(t)$ moves directly toward the path. When it reaches the path, it gradually accelerates to achieve the desired velocity. The control effort $|u_1(t)| + |u_2(t)|$ of path-following feedback law (c) is significantly lower than the control effort of tracking feedback law (a), Fig 1d. \square

III. PATH-FOLLOWING REDESIGN OF TRACKING FEEDBACK LAWS FOR REDUCTION OF CONTROL EFFORT

In this section we develop an algorithm for control effort reduction of tracking feedback laws for nonlinear systems

$$\dot{x} = f(x) + g(x)v, \quad x \in \mathbb{R}^n, \quad f(0) = 0, \quad (7)$$

$$y = h(x), \quad y, v \in \mathbb{R}^m, \quad h(0) = 0, \quad (8)$$

with stable zero dynamics and uniform vector relative degree $\{r, \dots, r\}$. For simplicity we assume the knowledge of a global diffeomorphism $T: \mathbb{R}^n \rightarrow \mathbb{R}^n$

$$\begin{bmatrix} z^T & \Xi^1 T & \dots & \Xi^m T \end{bmatrix}^T = T(x), \quad (9)$$

$z \in \mathbb{R}^{n-rm}$, $\Xi^i \in \mathbb{R}^r$, and a feedback transformation $v = \chi(x)u + \psi(x)$ [5], which transforms system (7)–(8) into

$$\dot{z} = \eta(z, \Xi), \quad \Xi \triangleq [\Xi^1 T \ \dots \ \Xi^m T]^T, \quad (10)$$

$$\dot{\Xi}^i = A_r \Xi^i + B_r u_i, \quad \Xi^i \triangleq [\xi_1^i \ \dots \ \xi_r^i]^T, \quad (11)$$

$$y_i = \xi_{r_1}^i, \quad i = 1, \dots, m, \quad (12)$$

where $u \triangleq [u_1 \ \dots \ u_m]^T$, $y \triangleq [y_1 \ \dots \ y_m]^T$, and $\eta(0, 0) = 0$. Subsystem (10) represents the zero dynamics assumed to be ISS with respect to Ξ as the input, so that boundedness of $z(t)$ is implied by boundedness of $\Xi(t)$. This allows us to disregard zero dynamics (10) from further considerations. Subsystem (11) represents m chains of r integrators, where states of the i^{th} chain are denoted by Ξ^i , $i = 1, \dots, m$.

Our problem for system (10)–(12) is to design a feedback law for u to enforce the geometric and dynamic tasks while guaranteeing boundedness of all closed-loop signals. The geometric task is to ensure that output y converges to geometric path $Y_P \triangleq \{y_P(\theta) = [y_{P1} \ \dots \ y_{Pm}]^T : \theta \in \mathbb{R}\}$, $y_{Pi}(\cdot) \in C^r$, $i = 1, \dots, m$, that is,

$$\lim_{t \rightarrow \infty} \|y(t) - y_P(\theta(t))\| = 0. \quad (13)$$

The dynamic task is to ensure that y moves along the path Y_P according to a given assignment, such as, *time*

assignment $\lim_{t \rightarrow \infty} |\theta(t) - v_t(t)| = 0$, and *speed assignment* $\lim_{t \rightarrow \infty} |\dot{\theta}(t) - v_s(\theta(t), t)| = 0$. Throughout this paper, without loss of generality, we assume that the dynamic task is given by the speed assignment $v_s(\theta, t) = v_0$.

The above path-following problem can be recast into the reference tracking framework by simultaneously enforcing the dynamic and geometric tasks. This is achieved by constructing a feedback law for u to track a fictitious reference signal $y_T(t) = [y_{T1}(t) \dots y_{Tm}(t)]^T \triangleq y_P(v_0 t + t_0)$, where t_0 is an arbitrary constant. With tracking error coordinates

$$\begin{aligned} e_T^T &\triangleq \Xi - Y_T = [e_{T1}^T \dots e_{Tm}^T]^T, & Y_T^T &\triangleq [Y_{T1}^T \dots Y_{Tm}^T]^T, \\ e_T^i &\triangleq \Xi^i - Y_{Ti} = [\xi_1^i - y_{Ti} \dots \xi_1^{i(r-1)} - y_{Ti}^{(r-1)}], \end{aligned}$$

subsystem (11) can be rewritten as $\dot{e}_T^i = A_r e_T^i + B_r(u_i - y_{Ti}^{(r)})$, $i = 1, \dots, m$. Therefore, a tracking feedback law

$$u = \kappa(e_T, y_T^{(r)}) \triangleq -K_g e_T + y_T^{(r)}, \quad (14)$$

where $K_g = \text{diag}(K_g^1, \dots, K_g^m)$, and K_g^i is chosen such that $A_r - B_r K_g^i$ is a Hurwitz matrix, solves the geometric and the dynamic task.

To develop a path-following solution to the above problem, we introduce the geometric error coordinates $e_P = [e_P^1 \dots e_P^m]^T \triangleq \Xi - Y_P(\theta, \dot{\theta})$, $e_P^i \triangleq \Xi^i - Y_P^i$, and the dynamic error coordinates $e_{\dot{\theta}} \triangleq \dot{\theta} - [v_0 \ 0 \dots 0]^T$, where

$$\begin{aligned} \Xi^i &\triangleq [\xi_1^i \dots \xi_1^{i(r-1)}]^T, & Y_P^i &\triangleq [y_{P1}^i \dots y_{P1}^{i(r-1)}]^T, \\ Y_P^T &\triangleq [Y_P^1 \dots Y_P^m]^T, & \dot{\theta} &\triangleq [\dot{\theta} \dots \dot{\theta}^{(r-1)}]^T. \end{aligned} \quad (15)$$

Substituting (15) into system (11)–(12) we obtain

$$\dot{e}_P^i = A_r e_P^i + B_r(u_i - y_{Pi}^{(r)}), \quad (16)$$

$$\dot{e}_{\dot{\theta}} = A_{r-1} e_{\dot{\theta}} + B_{r-1} \omega, \quad (17)$$

$$y_{ei} = e_{P1}^i, \quad i = 1, \dots, m. \quad (18)$$

As in system (4)–(5), $y_P^{(r)}$ gives rise to $r - 1$ new states $e_{\dot{\theta}}$ and $\theta^{(r)} \triangleq \omega$ becomes an additional control input. Then the geometric task is to render $e_{Pe} \triangleq 0$ GAS for *geometric error subsystem* (16) by a feedback law for u , while the dynamic task is to render $e_{\dot{\theta}e} \triangleq 0$ globally attractive for *dynamic error subsystem* (17) by a feedback law for ω .

Given a tracking feedback law $u = \kappa(e_T, y_T^{(r)})$, we use its corresponding path-following feedback law $u = \kappa(e_P, y_P^{(r)})$ to control the follower. Due to this correspondence, the properties of tracking feedback law (14) with respect to the reference signal y_T , are also the properties of the corresponding path-following feedback law with respect to the path y_P . Thus, the geometric task is enforced by selecting

$$u = \kappa(e_P, y_P^{(r)}) = -K_g e_P + y_P^{(r)}, \quad (19)$$

since the derivative of the Lyapunov function $V_g(e_P) = \sum_{i=1}^m e_P^T P_i e_P^i$, where $P_i = P_i^T > 0$, $i = 1, \dots, m$, solves $(A_r - B_r K_g^i)^T P_i + P_i (A_r - B_r K_g^i) = -I$, satisfies $\dot{V}_g \leq -\|e_P\|^2$ along the solutions of (16) and (19).

We decompose follower's feedback law (19) into four parts

$$\kappa = \kappa_g + \kappa_d + \kappa_{ss} + \frac{\partial y_P}{\partial \theta} \omega. \quad (20)$$

where $\kappa_g(e_P) \triangleq \kappa(e_P, y_P^{(r)}) - \kappa(0, y_P^{(r)})$ is the geometric, $\kappa_d(e_{\dot{\theta}}, \theta, t) \triangleq y_P^{(r)}|_{\omega=0} - \kappa_{ss}(\theta, t)$ is the dynamic, and

$\kappa_{ss}(\theta, t) \triangleq y_P^{(r)}|_{\omega=0, e_{\dot{\theta}}=0}$ is the steady-state part of feedback law (19). The only remaining degree of freedom in feedback law (19) is $\frac{\partial y_P}{\partial \theta} \omega$. Relying on this term we design a feedback law for ω to reduce the control effort of (19). However, the same feedback law is to solve the dynamic task. When V_g is large, that is, when the follower is far from the leader, the dominant part of the control signal comes from κ_g , and we design a feedback law for ω to reduce it. When V_g is small, the feedback law for ω is to enforce the dynamic task.

We obtain the feedback law for $\omega = \sigma(e_P, e_{\dot{\theta}}, \theta)$ by

$$\begin{aligned} \sigma(e_P, e_{\dot{\theta}}, \theta) &\triangleq \arg \min_{\omega} E_g(e_P, \theta, \omega) + c E_d(e_{\dot{\theta}}, \omega), \\ E_g(e_P, \theta, \omega) &\triangleq V_g(e_P) \|\kappa_g(e_P) + \frac{\partial y_P}{\partial \theta} \omega\|^2, \\ E_d(e_{\dot{\theta}}, \omega) &\triangleq (\omega + K_d e_{\dot{\theta}})^2, \end{aligned} \quad (21)$$

where $c > 0$ and K_d is chosen such that $A_{r-1} - B_{r-1} K_d$ is a Hurwitz matrix. This leads to

$$\sigma = -\frac{1}{c + \|\frac{\partial y_P}{\partial \theta}\|^2 V_g} \left(V_g \frac{\partial y_P}{\partial \theta}^T \kappa_g + c K_d e_{\dot{\theta}} \right). \quad (22)$$

The term E_g penalizes the geometric part of feedback law (19) and it contains V_g to increase its importance when the follower is far from the leader. The term E_d penalizes the difference between ω and a stabilizing feedback law for subsystem (17). By adjusting the constant c , feedback law (22) provides a tradeoff between the importance of enforcing the dynamic task and reducing the control effort of feedback law (19). Since $\lim_{t \rightarrow \infty} e_P(t) = 0$, we get that $\lim_{t \rightarrow \infty} \sigma(e_P(t), e_{\dot{\theta}}(t), \theta(t)) = -K_d e_{\dot{\theta}}(t)$, and thus, feedback law (22) solves the dynamic task. We note that (22) is well defined for all sufficiently smooth paths y_P and its magnitude is inversely proportional to $\|\frac{\partial y_P}{\partial \theta}\|$.

Leader's initial conditions $\theta(0)$ and $\dot{\theta}(0)$ significantly affect the control effort of feedback law (19), (22). We select them by minimizing the initial value of V_g

$$[\theta(0) \ \dot{\theta}(0)]^T = \arg \min_{s, \dot{s}} V_g(\Xi(0) - Y_P(s, \dot{s})). \quad (23)$$

The function $V_g(\Xi(0) - Y_P(\cdot, \cdot))$ is path dependent and may have several local minima, but based on follower's initial conditions $\Xi(0)$ it is often possible to provide a good initial estimate for its global minimizer.

This completes our algorithm. It is straightforward to extend it to uncertain triangular systems

$$\dot{\xi}_i = f_i(\xi_1, \dots, \xi_i) + \xi_{i+1}, \quad f_i(0) = 0,$$

where $y = \xi_1$, $\xi_i \triangleq [\xi_1^i \dots \xi_i^m]^T$, and functions f_i are given in terms of their bounds σ_{ij} , $\|f_i(\xi_1, \dots, \xi_i)\| \leq \sum_{j=1}^i \|\xi_j\| \sigma_{ij}(\xi_1, \dots, \xi_i)$, $i = 1, \dots, r$, $u \triangleq \xi_{r+1}$, but we do not pursue this direction here.

Example 2: We compare the control effort of path-following feedback law (19), (22) with control efforts of its corresponding tracking feedback law and the corresponding path-following feedback law designed in [4].

For system (1), the circular path $y_P(\theta) = R[\sin \theta \ \cos \theta]^T$, and the speed assignment $v_s(\theta, t) = v_0$, we design three feedback laws to enforce the geometric task, $\lim_{t \rightarrow \infty} y(t) - y_P(\theta(t)) = 0$, and the dynamic task, $\lim_{t \rightarrow \infty} \dot{\theta}(t) - v_0 = 0$.

Introducing geometric and dynamic error coordinates (15) into system (1), we solve the geometric task by selecting

$$u = \kappa_g + \kappa_d + \kappa_{ss} + \frac{\partial y_P}{\partial \theta} \omega, \quad (24)$$

where $\kappa_g \triangleq -K_g e_P$, $\kappa_d \triangleq \frac{\partial^2 y_P}{\partial \theta^2} e_{\dot{\theta}} (e_{\dot{\theta}} + 2v_0)$, $\kappa_{ss} \triangleq \frac{\partial^2 y_P}{\partial \theta^2} v_0^2$, and K_g is chosen such that $A_{2,2} - B_{2,2}K_g$ is Hurwitz. We satisfy the dynamic task by defining a feedback law for ω via (22), where $V_g(e_P) = e_P^T P e_P$ and $P = P^T > 0$ solves $(A_{2,2} - B_{2,2}K_g)^T P + P(A_{2,2} - B_{2,2}K_g) = -I$.

The corresponding tracking feedback law is given by (24), $\omega = 0$ and $\dot{\Theta}(0) = v_0$. To design the feedback law using the algorithm in [4], we redefine the geometric error coordinates

$$\begin{aligned} \tilde{e}_P &\triangleq \Xi - \tilde{Y}_P(\theta, v_0), \\ \tilde{Y}_P(\theta, v_0) &= [y_{P1} \frac{\partial y_{P1}}{\partial \theta} v_0 \ y_{P2} \frac{\partial y_{P2}}{\partial \theta} v_0]^T. \end{aligned} \quad (25)$$

The coordinates e_P in (15) and \tilde{e}_P in (25) differ in $\tilde{Y}_P(\theta, v_0)$. Namely, whenever $\dot{\theta}$ appears in (15), it is replaced by v_0 in (25). Consequently the highest derivative of θ appearing in (25) is $\dot{\theta} = \omega$, and it is treated as the control input. In coordinates (25) the dynamic and geometric tasks are coupled, forcing the simultaneous design of feedback laws for u and ω . It can be shown that the derivative of $V_g(\tilde{e}_P) = \tilde{e}_P^T P \tilde{e}_P$ along the solutions of (1) and the feedback law

$$u = -K_g \tilde{e}_P + \frac{\partial^2 y_P}{\partial \theta^2} v_0^2, \quad \omega = v_0 + g^T(\theta, v_0) P \tilde{e}_P, \quad (26)$$

where $g = \left[\frac{\partial y_{P1}}{\partial \theta} v_0 \ \frac{\partial^2 y_{P1}}{\partial \theta^2} v_0 \ \frac{\partial y_{P2}}{\partial \theta} v_0 \ \frac{\partial^2 y_{P2}}{\partial \theta^2} v_0 \right]^T$, satisfies $\dot{V}_g \leq -\|\tilde{e}_P\|^2$. This implies $\lim_{t \rightarrow \infty} \tilde{e}_P(t) = 0$ and $\lim_{t \rightarrow \infty} \dot{\theta}(t) = v_0$, hence, feedback law (26) solves the geometric and the dynamic task for system (1).

All feedback laws in this example use the same gains K_g and differ only in the methodology used to control leader's motion $\theta(t)$. To compare the control efforts it is important to choose leader's initial conditions appropriately. For feedback law (24), leader's initial conditions $\theta(0)$, $\dot{\Theta}(0)$ are two-dimensional and we compute them using (23). Leader's initial condition in the tracking feedback law and feedback law (26) is only $\theta(0)$, which we set to the value computed in (23). We measure the control effort of a feedback law from an initial condition $X(0) = [x_1(0) \ \dot{x}_1(0) \ x_2(0) \ \dot{x}_2(0)]^T$ by

$$CE(X(0)) = \int_0^{T_\epsilon} u^2(t) dt, \quad (27)$$

where $T_\epsilon = \min_t \{t \geq 0 : \forall \tau \geq t, \|e_P(\tau)\| + \|e_{\dot{\theta}}(\tau)\| \leq \epsilon\}$, and $\epsilon > 0$ is a small number. In other words, the control effort from an initial condition $X(0)$ is \mathcal{L}_2 norm of the control signal $u(t)$ needed to transfer the state $X(0)$ to the ϵ -neighborhood of the desired trajectory. In Fig. 2 we

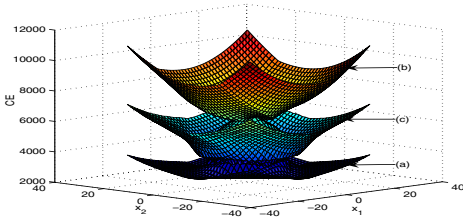


Fig. 2. Dependence of CE on $x_1(0)$ and $x_2(0)$ for: (a) feedback law (24), (22), (b) corresponding tracking feedback law, (c) feedback law (26).

show follower's control effort for the three feedback laws considered in this example, where K_g is computed in (3) for

$q = 100$, $r = 10$, $K_d = 2$ and $c = 100$. We project the function $CE(X(0))$ for $\epsilon = 0.1$ on the plane $\dot{x}_1(0) = 0$, $\dot{x}_2(0) = 0$, that is, we plot the dependence of the follower's control effort on its initial position, assuming that its initial velocity is zero. As observed in Fig. 2, the control effort of feedback law (24), (22), $CE_a(X(0))$, is significantly smaller for all initial conditions than the control efforts of its corresponding tracking feedback law, $CE_b(X(0))$, and feedback law (26), $CE_c(X(0))$. \square

IV. NONUNIFORM VECTOR RELATIVE DEGREE

Now we modify our path-following algorithm to make it applicable to systems (7) which have nonuniform vector relative degree $\{r_1, \dots, r_m\}$. Following the algorithm for systems with uniform vector relative degree, we obtain

$$\dot{e}_{\mathcal{P}}^i = A_{r_i} e_{\mathcal{P}}^i + B_{r_i} (u_i - y_{\mathcal{P}_i}^{(r_i)}), \quad i = 1, \dots, m, \quad (28)$$

$$\dot{e}_{\dot{\theta}} = A_{r^*-1} e_{\dot{\theta}} + B_{r^*-1} \omega, \quad (29)$$

$$y_e = [e_{\mathcal{P}_1}^1 \ \dots \ e_{\mathcal{P}_1}^m]^T, \quad (30)$$

where $\omega \triangleq \theta^{(r^*)}$, and $r^* \triangleq \max_i r_i$ is the largest relative degree of an output component $e_{\mathcal{P}_1}^i$ in (30), that is, the size of the longest integrator chain in (28). Note that $\omega = \theta^{(r^*)}$ appears only in chains L_{r^*} , where L_j denotes all integrator chains in (28) with length j , $L_j \triangleq \{i : r_i = j\}$, which represents the principal obstacle for applying the path-following algorithm from Section III to systems with nonuniform vector relative degree. Ignoring this obstacle and using (22) to define feedback law for ω results in reducing control effort of only feedback laws for u_i , $i \in L_{r^*}$, and may lead to undesirable closed-loop trajectories.

An option is to use dynamic extension [5], and add $r^* - r_i$ integrators to chains $i \notin L_{r^*}$. In other words, instead of solving the geometric task using static feedback laws for u_i , $i \notin L_{r^*}$, the dynamic feedback laws of the form

$$u_i^{(r^*-r_i)} = \kappa_i (e_{\mathcal{P}_i}^i, U_i, \theta, e_{\dot{\theta}}), \quad (31)$$

where $U_i \triangleq [u_i \ \dots \ u_i^{(r^*-r_i-1)}]^T$, are used. The extended system (28), (31) has uniform vector relative degree $\{r^*, \dots, r^*\}$ with respect to (30), and formula (22) is applicable. However, the resulting feedback law for ω reduces the control effort of $u_i^{(r^*-r_i)}$ instead of u_i , $i = 1, \dots, m$.

The alternative is to use dynamic reduction [8]. We split all chains of subsystem (28) into the upper part, with $r^\bullet \triangleq \min_i r_i$ integrators, and lower part, with $r_i - r^\bullet$ integrators, which gives rise to the following cascade system

$$\dot{\tilde{\Xi}}^i = A_{r^\bullet} \tilde{\Xi}^i + B_{r^\bullet} \tilde{u}_i, \quad \tilde{\Xi}^i \triangleq [\xi_1^i \ \dots \ \xi_{r^\bullet}^i]^T, \quad (32)$$

$$\dot{\tilde{U}}_i = A_{r_i - r^\bullet} \tilde{U}_i + B_{r_i - r^\bullet} u_i, \quad (33)$$

$$\dot{e}_{\dot{\theta}} = A_{r^*-1} e_{\dot{\theta}} + B_{r^*-1} \omega, \quad (34)$$

where $\tilde{u}_i \triangleq \xi_{r^\bullet+1}^i$, $\tilde{U}_i \triangleq [\tilde{u}_1 \ \dots \ \tilde{u}_i^{(r_i - r^\bullet)}]^T$, $i = 1, \dots, m$, $\tilde{u} \triangleq [\tilde{u}_1 \ \dots \ \tilde{u}_m]^T$. The upper part of the cascade, subsystem (32), has uniform vector relative degree $\{r^\bullet, \dots, r^\bullet\}$ with respect to (30), while the bottom part, subsystem (33), consists of integrator chains with variable length. Applying the algorithm from Section III to (32), we construct virtual feedback laws for \tilde{u} and $\theta^{(r^\bullet)}$

$$\tilde{u}_v = \kappa_v (\tilde{e}_P, \theta, \tilde{e}_{\dot{\theta}}), \quad \omega_v = \sigma_v (\tilde{e}_P, \theta, \tilde{e}_{\dot{\theta}}), \quad (35)$$

where \tilde{e}_P and \tilde{e}_Θ are defined by replacing r with r^\bullet in (15). This feedback law is not implementable since \tilde{u} , $\theta^{(r^\bullet)}$ are state variables of system (32)–(34), but we use backstepping to construct high-gain feedback laws for u and $\theta^{(r^\bullet)} = \omega$

$$u = \kappa(\tilde{e}_P, \tilde{U}, \theta, e_\Theta), \quad \omega = \sigma(\tilde{e}_P, \tilde{U}, \theta, e_\Theta), \quad (36)$$

where $\tilde{U} \triangleq [\tilde{U}_1 \dots \tilde{U}_m]^T$, to enforce fast convergence of $\tilde{u}(t)$ to $\tilde{u}_v(t)$, and $\theta^{(r^\bullet)}(t)$ to $\omega_v(t)$. By an appropriate choice of initial conditions $[\theta^{(r^\bullet)}(0) \dots \theta^{(r^\bullet-1)}(0)]^T$, it is possible to guarantee that $\theta^{(r^\bullet)}(t) \equiv \omega_v(t)$. We note that the feedback law for ω in (36) is designed to reduce the control effort of the virtual control $\tilde{u}_v(t)$, and its effectiveness in reducing the control effort of feedback law (36) depends on the convergence rate of $\tilde{u}(t)$ to $\tilde{u}_v(t)$.

V. CONTROL EFFORT REDUCTION OF TRACKING FEEDBACK LAWS FOR HOVERCRAFT

We illustrate our algorithm on a hovercraft model

$$\begin{aligned} \dot{x} &= u \cos \psi - v \sin \psi, & m\dot{u} - mvr + d_\nu u &= f_1, \\ \dot{y} &= u \sin \psi + v \cos \psi, & m\dot{v} + mur + d_\nu v &= 0, \\ \dot{\psi} &= r, & Jr + d_r r &= f_2, \end{aligned} \quad (37)$$

where x and y are the Cartesian coordinates of hovercraft's center of mass, u and v are surge and sway components of its velocity, ψ defines its orientation, and r is its angular velocity. Hovercraft's mass is denoted by m , its moment of inertia by J , f_1 is the pushing force, and f_2 is the steering torque. Friction is modelled by $d_\nu u$, $d_\nu v$ and $d_r r$, where $d_\nu, d_r > 0$. Hovercraft (37) exhibits a nonholonomic constraint because its sway velocity v can not be influenced instantaneously. When the output of interest is the position $p \triangleq [x \ y]^T$, hovercraft (37) does not have well-defined relative degree in any neighborhood of the origin, $0 \in \mathbb{R}^6$. Tracking problems for hovercraft are challenging, because most of the standard nonlinear tools, such as backstepping and feedback linearization, are not directly applicable. For more details on hovercraft and other underactuated vehicles see [6], [7] and references therein.

Given a path $y_P : \mathbb{R} \rightarrow \mathbb{R}^m$, a desired velocity v_0 along it, and two arbitrary constants $c_1, c_2 > 0$, our problem for hovercraft (37) is to design feedback laws for f_1 and f_2 which guarantee boundedness of all closed-loop trajectories and enforce the geometric task, $\limsup_{t \rightarrow \infty} \|p(t) - y_P(\theta(t))\| \leq c_1$, and to design a feedback law for the leader which enforces the dynamic task, $\limsup_{t \rightarrow \infty} |\dot{\theta}(t) - v_0| \leq c_2$. The relaxation of the geometric and dynamic tasks into their practical counterparts is a consequence of the nonholonomic constraint of the hovercraft.

Due to the space limitation, we omit the derivation of feedback laws for f_1 and f_2 , and only give their final expressions obtained by using the backstepping procedure from [6], [7]. To define these feedback laws we introduce several quantities: $e_{P1} \triangleq R^T(\psi)(p - y_P)$, $e_{P2} \triangleq [u \ v]^T - R^T(\psi)\dot{y}_P + \frac{k_1}{m}e_{P1}$, $\tilde{e}_{P2} \triangleq e_{P2} + [\frac{1}{m} \ 0]^T$, $\alpha \triangleq [\alpha_1 \ \alpha_2]^T = D_\nu \delta - h - \frac{1}{m}e_{P1} - \frac{k_2}{m}\tilde{e}_{P2}$, $h = (\frac{k_1}{m}D_\nu - \frac{k_1^2}{m})e_{P1} + k_1 e_{P2} - D_\nu R^T(\psi)\dot{y}_P - mR^T(\psi)\ddot{y}_P$, $e_{P3} \triangleq r - \alpha_2$, $D_\nu = \text{diag}(d_\nu, d_\nu)$, $n_1 = [1 \ 0]^T$, $n_2 = [0 \ 1]^T$, and

$$R(\psi) \triangleq \begin{bmatrix} \cos \psi & -\sin \psi \\ \sin \psi & \cos \psi \end{bmatrix}, \quad S(r) \triangleq \begin{bmatrix} 0 & -r \\ r & 0 \end{bmatrix}.$$

Using the Lyapunov function $V = \frac{1}{2}(\|e_{P1}\|^2 + \|\tilde{e}_{P2}\|^2 + e_{P3}^2)$ it can be shown [6], [7] that the feedback law

$$f_1 = \alpha_1, \quad f_2 = d_r \alpha_2 + J\dot{\alpha}_2 - mn_2^T \tilde{e}_{P2} - k_3 e_{P3}, \quad (38)$$

ensures boundedness of all closed-loop signals and guarantees that $\|p(t) - y_P(\theta(t))\| \leq p_0 e^{-\lambda t} + \epsilon$, where $p_0 > 0$ depends on initial conditions, and $\lambda, \epsilon > 0$. Furthermore, by selecting appropriate values for parameters k_1 , k_2 , and k_3 , any values of λ and ϵ can be obtained. Thus, feedback law (38) solves the geometric task for any $\theta(t)$.

Since the control input f_1 is separated by two integrators from the output p , the feedback law for f_1 in (38) is obtained via two steps of backstepping and the highest derivative of θ appearing in it is $\ddot{\theta}$. Similarly, the highest derivative of θ in the feedback law for f_2 in (38) is $\theta^{(3)}$. Thus, $\theta^{(3)} \triangleq \omega$ becomes a control input which is to ensure the dynamic task and reduce the control effort. Defining the dynamic error by $e_\Theta \triangleq [\dot{\theta} - v_0 \ \ddot{\theta}]^T$, the dynamic task is enforced by rendering $e_{\Theta_e} \triangleq [0 \ 0]^T$ globally practically attractive for

$$\dot{e}_\Theta = A_2 e_\Theta + B_2 \omega. \quad (39)$$

We first solve the dynamic task by designing a feedback law for ω via dynamic reduction. Since hovercraft's moment of inertia J is typically small, we decompose system (37) into a fast and a slow subsystem. The fast subsystem governs angular velocity r and it is controlled by steering torque f_2 . The slow subsystem consists of the remaining equations in (37), its relative degree is $\{2, 2\}$ (from p to $[f_1 \ r]^T$), and its virtual feedback law is $\alpha = [\alpha_1 \ \alpha_2]^T$. If J is not small, this time-scale separation is to be induced via the feedback law for f_2 by increasing the constant k_3 . Treating $\ddot{\theta} \triangleq \omega_v$ as a virtual control input into the slow subsystem, we define a feedback law for it via (21), which results in

$$\omega_v = -\frac{1}{c + V_2 \|\frac{\partial y_P}{\partial \theta}\|^2} \left(V_2 \frac{\partial y_P}{\partial \theta}^T R(\psi) \alpha_g + ck_{d1} e_\Theta \right), \quad (40)$$

where $k_{d1} > 0$, $V_2 = \frac{1}{2}\|e_{P1}\|^2 + \frac{1}{2}\|\tilde{e}_{P2}\|^2$, and $\alpha_g = (\frac{1}{m} + \frac{k_1}{m}D_\nu - \frac{k_1^2}{m})e_{P1} + (k_1 + \frac{k_2}{m})\tilde{e}_{P2}$ is the geometric part of α . Applying backstepping on ω_v , we obtain implementable feedback law for $\theta^{(3)} = \omega$

$$\omega = \frac{d\omega_v}{dt} - k^*(\ddot{\theta} - \omega_v), \quad k^* > 0, \quad (41)$$

which enforces the dynamic task for (39). Taking $\dot{\theta}(0) = \omega_v(0)$ we get $\dot{\theta}(t) \equiv \omega_v(t)$, while $\theta(0)$ and $\dot{\theta}(0)$ are computed from (23), where $V_g = V_2$.

For the dynamic extension approach, we first add an integrator to system (37). Namely, we design a feedback law for \dot{f}_1 instead of f_1 , which makes both control inputs, \dot{f}_1 and f_2 , separated by three integrators from the output p . Using the Lyapunov function $\tilde{V} \triangleq V_2 + \frac{1}{2}\tilde{e}_{P3}^T \tilde{J} \tilde{e}_{P3}$, $\tilde{J} \triangleq \text{diag}(1, J)$, $\tilde{e}_{P3} \triangleq [f_1 - \alpha_1 \ e_{P3}]^T$ it can be shown that feedback law

$$\dot{f}_1 = \dot{\alpha}_1 - mn_1^T \tilde{e}_{P2} - k_3(f_1 - \alpha_1), \quad (42)$$

coupled with the feedback law for f_2 in (38) solves the geometric task for hovercraft (37). Now we solve the dynamic task by applying formula (21), which results in

$$\omega = -\frac{\tilde{V} \frac{\partial y_P}{\partial \theta}^T R(\psi) \tilde{J} \tilde{K}_g + cK_d e_\Theta}{c + \tilde{V} \frac{\partial y_P}{\partial \theta}^T R(\psi) \tilde{J}^2 R^T(\psi) \frac{\partial y_P}{\partial \theta}}, \quad (43)$$

where $\tilde{\kappa}_g \triangleq J^2 \tilde{J}^{-1} \kappa_g$ is the scaled geometric part of feedback law (38), (42), $\kappa_g \triangleq \dot{\alpha}_g - m\tilde{e}_{\mathcal{P}2} + d_r \text{diag}(0, 1)\alpha_g - k_3 \tilde{e}_{\mathcal{P}3}$. Since J is typically small, without this scaling the geometric part of f_1 is drastically more penalized than the geometric part of f_2 , resulting in large ω and leader's fast motion along the path. The initial condition for feedback law (42) is set to $f_1(0) = \alpha_1(0)$, while leader's initial conditions, $[\theta(0) \dot{\theta}(0) \ddot{\theta}(0)]^T$, are computed via (23), where $V_g = \tilde{V}$.

In Figs. 3 and 4 we compare the typical behavior of the hovercraft system for: (a) tracking feedback law, (b) path-following feedback law developed in [4], (c) path-following feedback law (38), (41) obtained via dynamic reduction, (d) path-following feedback law (38), (42), (43) obtained via dynamic extension. The derivation of feedback law (b) omitted, while the tracking feedback law which correspond to (a) is given by (38), $\omega = 0$, $\dot{\theta}(0) = v_0$ and $\ddot{\theta}(0) = 0$.

We set the parameters to values for the actual hovercraft vehicle from Caltech's experimental testbed: $m = 5.15 \text{ kg}$, $J = 0.047 \text{ kgm}^2$, $d_\nu = 4.5 \text{ kg/s}$, and $d_r = 0.41 \text{ kgm/s}$, and adopt feedback parameters: $k_1 = 4$, $k_2 = 1.5$, $k_3 = 0.6$, from the tracking feedback law which was experimentally validated in [6]. The additional parameters for feedback laws (c), (d) are respectively: $c = 100$, $k_{d1} = 1$, $k^* = 10$, and $c = 100$, $K_d = [44]$. We consider a circular path with radius $R = 10 \text{ m}$, and let the desired velocity along it be $v_0 = 1 \text{ m/s}$. Hovercraft's initial conditions are: $X^*(0) = [p(0)^T \psi(0) u(0) v(0) r(0)]^T = [25 \ -25 \ 0 \ 0 \ 0]^T$. Leader's initial condition $\theta(0)$ for feedback laws (a), (b) is set to the value of $\theta(0)$ computed for feedback law (c).

In Fig. 3 we show the typical behavior and the control effort for feedback laws (a), (b). Since leader's motion $y_T(t) = y_{\mathcal{P}}(v_0 t + \theta(0))$ is predetermined for tracking feedback law (a) in Fig. 3i, the follower is forced to use large control effort to catch up with the leader. The peak value of the pushing force $f_1(t)$, which represents the dominant part of the control effort, is $\max_t |f_1(t)| = 172$. A significant reduction of control effort is achieved with path-following feedback law (b), Fig. 3ii, but the peak value of $f_1(t)$ is still large, $\max_t |f_1(t)| = 170$.

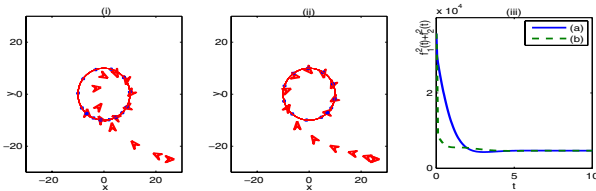


Fig. 3. Hovercraft's and leaders' positions, $p(t_i)$ and $y_{\mathcal{P}}(\theta(t_i))$, at $t_i = 0.6i$, and pointwise norm of the control signals, $f_1^2(t) + f_2^2(t)$ for: tracking feedback law (a), path-following feedback law (b).

In Fig. 4 we show the typical behavior and the control effort for feedback laws (c) and (d) developed in this paper. The motion of the leader $y_{\mathcal{P}}(\theta(t))$ has two phases. Initially the leader disregards the dynamic task, and waits at a "convenient place" for the follower to converge to it. Thus the follower does not waste the control effort to unnecessarily chase the leader. In the second phase the leader gradually accelerates to the desired speed. The tradeoff between the dynamic task and the control effort reduction is particularly

revealing in Fig. 4i. The peak values of $f_1(t)$ for feedback laws (c), (d) are $\max_t |f_1(t)| = 96$, $\max_t |f_1(t)| = 99$, respectively. The control effort from an initial condition $X(0)$ is measured by $CE(X(0)) = \int_0^{T_\epsilon} f_1^2(t) + f_2^2(t) dt$, where $T_\epsilon \triangleq \min_t \{t \geq 0 : \forall \tau \geq t, \|e_{\mathcal{P}1}(\tau)\| + \|e_{\mathcal{P}2}(\tau)\| + \|e_{\mathcal{P}3}(\tau)\| + \|e_{\dot{\theta}}(\tau)\| \leq \epsilon\}$, and $\epsilon = 0.2$. For simulations shown in Fig. 3 and 4, we get: $CE_a(X^*(0)) = 1.9 \times 10^4$, $CE_b(X^*(0)) = 3.5 \times 10^4$, $CE_c(X^*(0)) = 6.6 \times 10^4$, $CE_d(X^*(0)) = 3.8 \times 10^4$. The same ordering of control efforts, $CE_a < CE_b < CE_d < CE_c$, holds for all initial conditions for which we performed simulations.

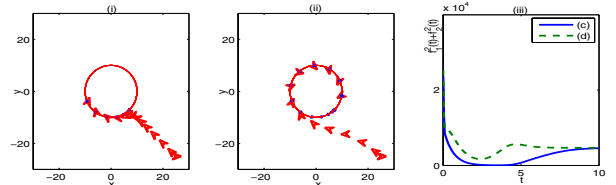


Fig. 4. Hovercraft's and leaders' positions, $p(t_i)$ and $y_{\mathcal{P}}(\theta(t_i))$, at $t_i = 0.6i$, and pointwise norm of the control signals, $f_1^2(t) + f_2^2(t)$ for path-following feedback laws obtained via: dynamic reduction (c), dynamic extension (d).

VI. CONCLUSION

In this paper we introduce a leader-follower methodology for design of path-following feedback laws. We first construct a feedback law for the follower to ensure its desired convergence rate to the leader for any leader's motion. This leaves leader's motion as an additional degree of freedom which we exploit to reduce follower's control effort. The price paid for this reduction is a delay in enforcing the dynamic task. We demonstrate the effectiveness of the developed path-following algorithm on a hovercraft model.

Although our algorithm does not explicitly account for input saturation, the resulting path-following feedback laws require less control effort and are likely to perform better in such situations than the corresponding tracking feedback laws. An explicit consideration of the input saturation is a focus of the current research.

REFERENCES

- [1] J. Hauser and R. Hindman, "Maneuver regulation from trajectory tracking: Feedback linearizable systems", *Proc. of IFAC Symp. on Nonlinear Control Systems Design*, Lake Tahoe, CA, USA, 1995.
- [2] P. Encarnação, A.M. Pascoal, "3D Path-following for Autonomous Underwater Vehicle", in *Proc. of 39th IEEE CDC*, Sydney, Australia, December 2000.
- [3] S.A. Al-Hiddabi and N.H. McClamroch, "Tracking and Maneuver Regulation for Nonlinear Nonminimum Phase Systems: Application to Flight Control", *IEEE Tran. on Control System Technology*, vol. 10, 2002, pp 780-792.
- [4] R. Skjetne, T.I. Fossen and P.V. Kokotović, "Robust Output Maneuvering for a Class of Nonlinear Systems", *Automatica*, vol. 40, pp. 373-383, 2004.
- [5] A. Isidori, "Nonlinear Control Systems", *Springer*, New York, 1997.
- [6] A.P. Aguiar, L. Cremean and J.P. Hespanha, "Position Tracking for a Nonlinear Underactuated Hovercraft: Controller Design and Experimental Designs", in *Proc. of 42nd IEEE CDC*, Maui, Hawaii, December 2003.
- [7] A.P. Aguiar and J.P. Hespanha, "Position Tracking of Underactuated Vehicles", in *Proc. of ACC*, Denver, Colorado, June 2003.
- [8] R. Sepulchre, M. Janković and P.V. Kokotović, "Constructive Nonlinear Control", *Springer-Verlag*, London, 1997.
- [9] J.W. Grizzle, M.D. Di Benedetto and F. Lamabhi-Lagarigue, "Necessary conditions for asymptotic tracking in nonlinear systems", *IEEE Tran. on Automatic Control*, Vol. 39, pp. 1782 -1794, 1994.